Dimensions of Luminescent Oxidized and Porous Silicon Structures

S. Schuppler,[1] S. L. Friedman,[1] M. A. Marcus,[1] D. L. Adler,[1,*] Y.-H. Xie,[1] F. M. Ross,[2] T. D. Harris,[1] W. L. Brown,[1] Y. J. Chabal,[1] L. E. Brus,[1] and P. H. Citrin[1]

[1]*AT&T Bell Laboratories, Murray Hill, New Jersey 07974*

[2]*National Center for Electron Microscopy, Lawrence Berkeley Laboratory, Berkeley, California 94720*

(Received 12 January 1994)

X-ray absorption measurements from H-passivated porous Si and from oxidized Si nanocrystals, combined with electron microscopy, ir absorption, α recoil, and luminescence emission data, provide a consistent structural picture of the species responsible for the visible luminescence observed in these samples. The mass-weighted average structures in por-Si are particles, not wires, with dimensions significantly smaller than previously reported or proposed.

PACS numbers: 78.70.Dm, 61.10.Lx, 61.46.+w, 78.55.−m

The novel properties and possible utility of visible room-temperature luminescence from anodically grown porous silicon (por-Si) have generated intense study [1], from which a growing consensus has emerged for explaining the luminescence with quantum-confined structures [2,3]. (Luminescence from por-Si passivated with O rather than H [4] has ruled out a SiH_x species, while the absence of Si-O bonding in x-ray absorption data from por-Si [5] has ruled out siloxenes.) There remains, however, a basic lack of knowledge regarding the dimensions and shape of the species actually responsible for the optical activity, largely because the material is inhomogeneous, but also because there is little direct structural information from the region lying within the penetration depth of the photoexciting radiation. Even for 80% porosity samples excited by ~350–400-nm light (where the luminescence is a maximum [5,6]), this depth is < 5000 Å [7] and thus not well suited for standard microscopy or diffraction techniques from as-prepared material. Moreover, Si structures < 20 Å, should they be significant, are beyond practical detection with these methods. Added to these experimental limitations are theoretical uncertainties in correlating band gap with Si size, where nanoscale particle or wire dimensions for a given gap vary by more than 100% [1,8].

We report on x-ray absorption measurements from a series of oxidized Si nanocrystals, whose shapes and sizes are known, and from a variety of anodically grown (H-passivated) por-Si samples. The data, combined with luminescence emission measurements from each of the systems, establish new and unexpectedly smaller values for the average size of Si structures contained within optically relevant depths of por-Si. In addition, the general importance of extended wire shapes is ruled out. Our results have significant implications for describing the origin of visible photoluminescence from por-Si.

The Si K-edge absorption measurements were performed at the National Synchrotron Light Source using the AT&T X15B beam line [9] and InSb(111) monochromating crystals. Samples were kept at 77 K to minimize thermal disorder effects [10]. All data were obtained with total electron yield detection, whose effective sampling depth in 80% porosity Si is < 2500 Å [11]. A variety of por-Si samples prepared under very different conditions [12] were studied with transmission electron microscopy (TEM), x-ray and ir absorption, α recoil, and luminescence excitation and emission spectroscopies. Air exposure of the freshly prepared samples was limited to < 10 min in all but the TEM measurements to minimize O contamination (such effects were easily detectable). Samples of the O-passivated (air-insensitive) Si nanocrystals [13] were prepared for x-ray absorption measurements by transferring them as colloidal suspensions onto graphite substrates.

In Fig. 1(a) we show Si K near-edge x-ray absorption fine structure (NEXAFS) data from three different sizes of oxidized Si (ox-Si) nanocrystals, ox-Si_x, labeled small (s), medium (m), and large (l). A fourth, very small (vs) sample was also measured but omitted in Fig. 1(a) for clarity. Comparison with data from c-Si (freshly HF rinsed to remove the native oxide film) and bulk SiO_2 readily confirms that these are the two main components in the clusters [14]. The c-Si, SiO_2, and ox-Si_x data have been normalized to common "edge jump" values measured > 100 eV above the Si K edge where their x-ray absorption intensities are structureless, i.e., atomiclike. The relative concentrations of Si and SiO_2 in the nanocrystals are directly proportional to their individual, easily separable edge jumps [10]. Now, x-ray diffraction, liquid chromatography, and TEM data [13] show that the l, m, s, and vs samples are SiO_2-coated spheres of Si whose outer diameters are 96 ± 19, 45 ± 7, 33 ± 6, and 26 ± 6 Å, respectively. From these values, the spherical shapes, and the measured relative concentrations of Si and SiO_2, we determine the mean inner diameters of the corresponding Si cores to be 81, 31, 17, and 12 Å. These nanocrystal sizes are plotted as circles in the bottom half of Fig. 2 versus their measured peak luminescence energies. The high quantum efficiencies of these particles (> 25% at low temperatures [13]), the essentially constant oxide thicknesses found here (7–8 Å) for very different diameters, and the well defined trend seen in the

0031-9007/94/72(16)/2648(4)$06.00

© 1994 The American Physical Society

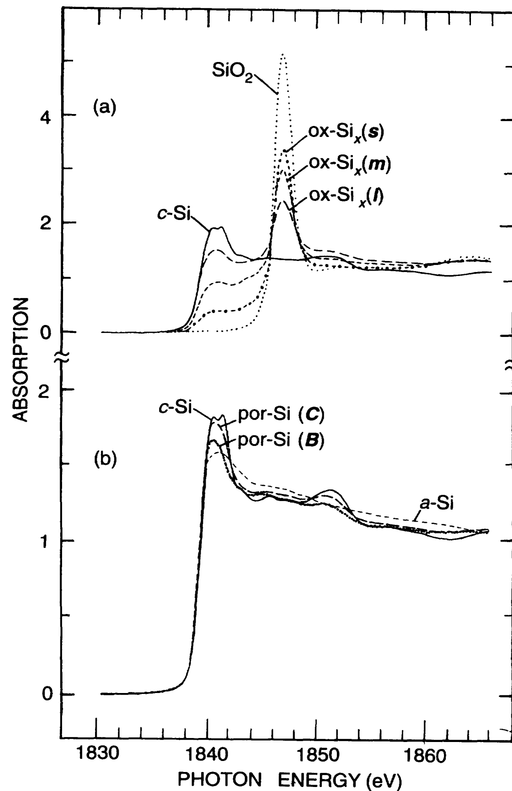

FIG. 1. (a) Si K-edge NEXAFS data from c-Si, SiO_2, and oxidized Si nanocrystals of different size, labeled small (s), medium (m), and large (l). (b) NEXAFS data from c-Si, a-Si, and two differently prepared por-Si samples. All data in (a) and (b) are normalized to unity edge jump.

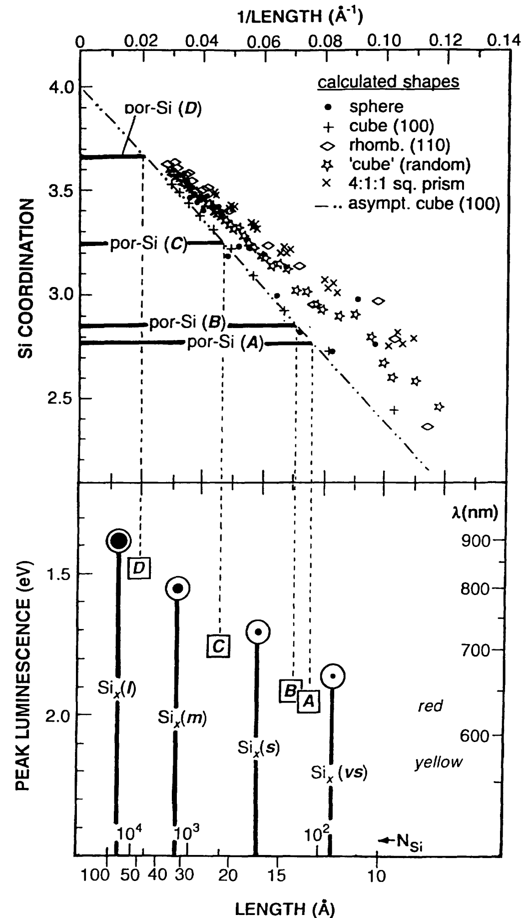

FIG. 2. Top: Correlation between average Si coordination for particles of different shapes versus their inverse characteristic lengths (diameter for sphere, side for cube or rhombus). Average includes bulk and surface atoms, which have < 4 first neighbors, explaining trend of lower values with decreasing particle size. Experimental Si coordinations from EXAFS data of four differently prepared por-Si samples labeled A, B, C, and D are indicated. Bottom: Correlation between average Si particle size and measured peak luminescence energy. Also indicated is the total number of Si atoms, N_{Si}, contained in a cubic particle of corresponding size. Different sized oxidized Si nanocrystals labeled vs, s, m, and l are shown as circles; different por-Si structures from top figure are shown as squares.

bottom of Fig. 2 all clearly identify the Si_x cores as the optically active species in these samples.

Normalized NEXAFS data from por-Si appear in Fig. 1(b), along with comparison data from c-Si and HF-rinsed a-Si. For clarity, we show only two of the four differently prepared samples studied here [12], labeled C [2] and B [5]. The lack of (Si-O)-related absorption at ~1842–1848 eV, and the qualitatively closer resemblance to c-Si than to a-Si, are apparent. More detailed information can be obtained from the corresponding extended x-ray absorption fine structure (EXAFS) data and their analysis [10] in Fig. 3. Locally ordered structure in the por-Si samples is seen from the second- and third-neighbor shells appearing as peaks at ~3.4 and 4.1 Å in the Fourier-transformed (FT) data [Fig. 3(b)]; such structure in a-Si is essentially absent, of course, due to static disorder. Relative to bulk c-Si, the apparently similar reduction of first-neighbor FT peak intensities at ~2.0 Å for the por-Si and a-Si samples is better understood by filtering and backtransforming the first-neighbor shells [Fig. 3(c)]. The peak intensity of the amplitude function $A(k)$, which envelopes the oscillatory EXAFS $\chi(k)$, is shifted for a-Si as a result of the Debye-Waller-like static-disorder term [10]. Such exponential damping of high-k scattering is unimportant for $k < 4$ Å^{-1}, so in that region $A(k)$ for the a-Si and c-Si samples is the same. This reflects their identical Si coordinations of 4. By contrast, $A(k)$ for the por-Si samples is *unshifted* relative to that for c-Si and is *smaller* at *all* values of k. This is an obvious indication that the average number of first-neighbor Si atoms, $\mathcal{N}_{Si}$, in por-Si is < 4.

The reason for the lower average Si coordination number and the apparent lack of other first neighbors in the FT data is that the surface Si atoms are also coordinated to H (the EXAFS backscattering amplitude of H is negli-

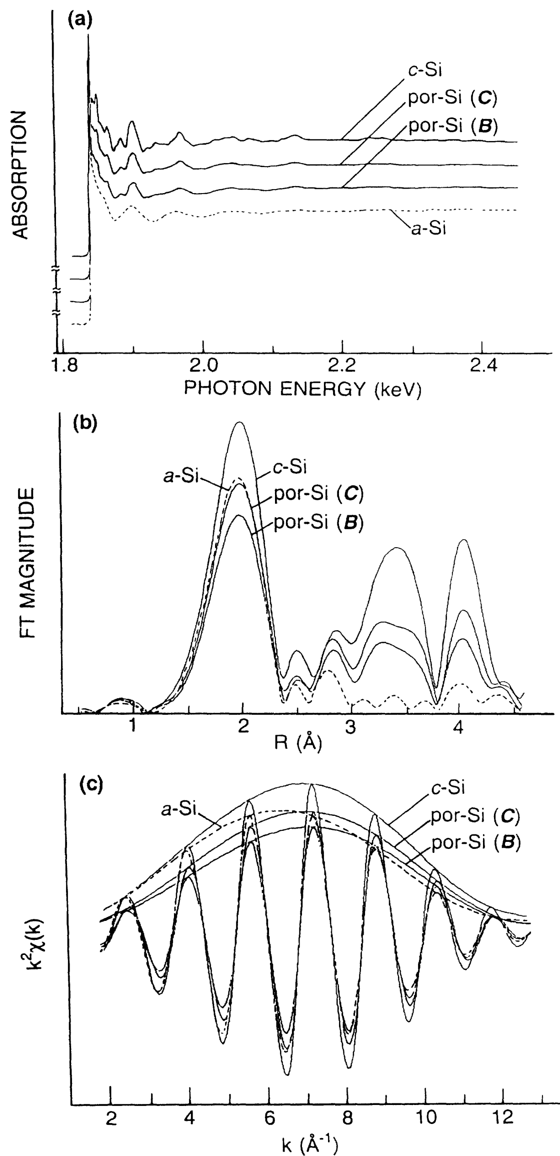

FIG. 3. (a) Raw Si K-edge EXAFS data from c-Si, a-Si, and two differently prepared por-Si samples. (b) Fourier transforms of edge-truncated, k^2-multiplied, background-subtracted data from samples in (a). First-, second-, and third-shell peaks at $\sim$2.0, 3.4, and 4.1 Å are uncorrected for phase shift. Artifactual peaks at $\sim$2.5 and 2.9 Å are due to truncation. (c) Back-transformed, filtered first-shell data from (b).

gible). The substantially smaller values of $\mathcal{N}_{\mathrm{Si}}$ obtained by fitting [10] the filtered por-Si data indicate large H/Si ratios in these samples. For example, $\mathcal{N}_{\mathrm{Si}}=2.85\pm0.1$ in sample B, meaning H/Si$=1.15\pm0.1$, or an average H content of 115%. This should be compared with typical H concentrations of $\sim$10% in device-quality a-Si:H [15]. Forward α-recoil measurements [16], which determine H/Si directly, give results for the corresponding por-Si samples that are fully consistent with those from EXAFS. Furthermore, these integrated H concentrations are confirmed by transmission ir-absorption measurements [17] (the ir results also show that H from bulk Si or from possible OH contamination is unimportant in the α-recoil data).

The large measured H/Si ratios imply large surface/volume ratios for the representative Si structures, the average sizes of which are determined in the top half of Fig. 2. We first plot calculated Si coordinations for different shapes as a function of inverse characteristic dimension, or length (i.e., diameter for a sphere, side for a cube or rhombus). The dot-dashed line, drawn from the asymptotic limit of $\mathcal{N}_{\mathrm{Si}}=4$ for infinitely large Si dimensions, is extended for (100)-faceted cubic particles of decreasing size. The 4:1:1 square-prism shapes are included to represent prolate particles. All particle surfaces (terminated with H) are ideal. To this calculated plot we then indicate the Si coordinations measured from the EXAFS amplitudes in the four different por-Si samples, labeled A, B, C, and D (all $\mathcal{N}_{\mathrm{Si}}$ values are ±0.1). Finally, the average Si particle sizes are obtained from the intersection of mean experimental Si coordinations with the asymptotic dot-dashed line. These sizes are plotted as squares in the bottom half of Fig. 2 against the peak luminescence energies measured in the corresponding samples. A correlation is obvious.

Before discussing this trend, we point out that the particle sizes represented by the squares are actually *upper limits*. The quoted particle sizes are obtained from the (100)-cubic asymptote, so any other assumed shape(s) would clearly lead to smaller sizes. Furthermore, TEM micrographs of the por-Si samples show them to contain regions of unetched c-Si whose dimensions are substantially larger than 3 nm and whose amounts vary between 10% and 20% depending on the type of sample studied. These unetched regions separate areas of por-Si structures too small to characterize easily with TEM. Since EXAFS measurements average over *all* the Si structures, including the contributions from c-Si, the reduced values quoted for $\mathcal{N}_{\mathrm{Si}}$—and thus the mass-weighted average particle sizes—would be even smaller had these larger unetched c-Si contributions not been included.

The bottom of Fig. 2 displays the important and surprising result that the relationship between peak luminescence energy and average particle size for the por-Si samples is very similar to that for the Si nanocrystals. Indeed, excluding the unetched contributions in our data analysis for obtaining values of $\mathcal{N}_{\mathrm{Si}}$ would make the two trends virtually indistinguishable. The implication is clear: Since the luminescence spectrum from a given Si nanocrystalline particle is directly correlated with its size, the luminescence spectrum from a given por-Si sample is also associated with a characteristic Si dimension. Thus, for example, 720-nm peak luminescence from Si is representative of a structure whose average size is $\sim$20 Å, *regardless of how the sample was prepared.*

The correlation in Fig. 2 also provides information about the shape of the Si species responsible for the

luminescence in the visible region <700 nm (>1.75 eV). If extended, wirelike shapes with aspect ratios $\gg 4{:}1$ were responsible for the luminescence in these samples, they would have to be of extremely small dimensions, <10 Å. This implies, therefore, that the optically active structures are generally not extended wires, but particles. We infer that these particles are predominantly (100) faceted based on surface sensitive reflection ir-absorption measurements [18] from the por-Si *A* and *B* samples, which indicate H-Si frequencies representative of SiH_2 species [(110) or (111) surfaces would exhibit frequencies associated mainly with SiH]. More general conclusions cannot be extended to samples luminescing in the near- and far-infrared region, i.e., >700 nm, because the distinction between wires and particles (see Fig. 2) is less significant.

The average sizes of the Si structures responsible for the *visible* luminescence in por-Si are small, well below easy detection with TEM or diffraction. For example, Fig. 2 indicates that 2-eV luminescence is associated with particles of dimensions typically less than 13 Å (recall that the values shown in squares are upper limits). This is considerably smaller than any size previously associated with such luminescence. A 13-Å cube contains a total number of Si atoms $N_{Si} \approx 110$ (≈ 60 for a sphere [19]; see Fig. 2) and a calculated band gap of ~ 3.8 eV [8], whereas a 26-Å cube has corresponding numbers of ~ 900 and 2.2 eV. Factors of 2 in size are therefore very important.

Basic questions about visible photoluminescence from por-Si still remain. Among these are the possible role of defect states and radiative traps in determining overall quantum efficiencies. A complete description of the visible-luminescence mechanism in por-Si will ultimately need to address these issues, along with the fact that the optically active Si species in this material has dimensions as small as those found here.

We are indebted to E. E. Chaban and P. J. Szajowski for valuable technical contributions. S. Schuppler is grateful to the Alexander von Humboldt Foundation for financial support. The EXAFS experiments were performed at the NSLS, Brookhaven National Laboratory, which is supported by the DOE, Division of Materials Sciences and Division of Chemical Sciences. The TEM measurements, performed at the National Center for Electron Microscopy, LBL, are supported by the Director, Office of Basic Energy Sciences, DOE, under Contract No. DEAC03-76SF00098.

*Present address: Department of Material Science, University of Illinois at Urbana-Champaign, Urbana-Champaign, IL 61801.

[1] For example, see Mater. Res. Soc. Proc. **256** (1992); **283** (1993); **298** (1993).

[2] L. T. Canham, Appl. Phys. Lett. **57**, 1046 (1990).

[3] V. Lehmann and U. Gösele, Appl. Phys. Lett. **58**, 856 (1991).

[4] V. Petrova-Koch, T. Muschik, A. Kux, B. K. Meyer, and F. Koch, Appl. Phys. Lett. **61**, 943 (1992).

[5] S. L. Friedman, M. A. Marcus, D. L. Adler, Y.-H. Xie, T. D. Harris, and P. H. Citrin, Appl. Phys. Lett. **62**, 1934 (1993).

[6] Y. H. Xie, M. S. Hybertsen, W. L. Wilson, S. A. Ipri, G. E. Carver, W. L. Brown, E. Dons, B. E. Weir, A. R. Kortan, G. P. Watson, and A. J. Liddle, Phys. Rev. B **49**, 5386 (1994); Y.-H. Xie (unpublished).

[7] D. E. Aspnes and A. A. Studna, Phys. Rev. B **27**, 985 (1983). Depths have been crudely estimated by multiplying by 5 to account for the 80% porosity.

[8] See, e.g., C. Delerue, G. Allan, and M. Lannoo, Phys. Rev. B **48**, 11 024 (1993), and references therein.

[9] A. A. MacDowell, T. Hashizume, and P. H. Citrin, Rev. Sci. Instrum. **60**, 1901 (1989).

[10] P. A. Lee, P. H. Citrin, P. Eisenberger, and B. M. Kincaid, Rev. Mod. Phys. **53**, 769 (1981).

[11] A. Erbil, G. S. Cargill, R. Frahm, and R. F. Boehme, Phys. Rev. B **37**, 2450 (1988).

[12] Preparations of the por-Si samples studied here (called *A*, *B*, *C*, and *D*) follow those in Refs. [2], [5], and [6], namely, *C* [2]: *p*-type Si(100), >50 Ω cm, 20% HF in alcohol, 20 mA/cm^2 for 5 min; *A* [6]: same as *C*, but etched 60 min; *B* [5]: *p*-type Si(100), >50 Ω cm, 15% HF in alcohol, 25 mA/cm^2 for 12 min; *D* [5]: *p*-type Si(100), 0.5–0.8 Ω cm, 40% HF in alcohol, 50 mA/cm^2 for 80 sec, soaked 2 h unetched in same solution.

[13] Oxidized Si nanocrystals were made by homogeneous nucleation in high-pressure He at 1000 °C from thermal decomposition of disilane with subsequent oxidation in O_2 at 1000 °C for ~ 30 msec. See K. A. Littau, P. J. Szajowski, A. J. Muller, A. R. Kortan, and L. E. Brus, J. Phys. Chem. **97**, 122 (1993); W. L. Wilson, P. J. Szajowski, and L. E. Brus, Science **262**, 1242 (1993); P.J. Szajowski and L. E. Brus (unpublished).

[14] The interfacial SiO_x component measured in all four samples is ~ 1 monolayer thick.

[15] R. A. Street, *Hydrogenated Amorphous Silicon* (Cambridge University Press, Cambridge, 1991).

[16] B. L. Cohen, C. L. Fink, and J. H. Degnan, J. Appl. Phys. **43**, 19 (1972).

[17] The volumes used for integrating the measured SiH_x concentrations in the por-Si samples were obtained from TEM.

[18] Surface sensitivity of <1 μm was obtained using a grazing internal incidence angle in a Ge plate positioned next to the por-Si samples.

[19] For a Si cube of side L, $N_{Si} = 8L^3/a_0^3$; for a sphere of diameter L, $N_{Si}^{sph} = (\pi/6)N_{Si}^{cube}$.